NUMERICAL MODELING OF ELEMENTARY BENDING-ACTIVE STRUCTURES: BEAM, GRIDSHELL, AND UMBRELLA

Amber Y. Lin

amberl@princeton.edu

Department of Civil and Environmental Engineering – Princeton University

59 Olden Street, 08544, NJ, Princeton, United States

Ruy M.O. Pauletti

pauletti@us.br

Departamento de Engenharia de Estruturas e Geotécnica – Escola Politécnica da USP

Av. Prof. Almeida Prado, trav. 2, 271 - 05508-900 - São Paulo – SP, Brasil

Sigrid Adriaenssens

sadriaen@princeton.edu

Department of Civil and Environmental Engineering – Princeton University

59 Olden Street, 08544, NJ, Princeton, United States

Abstract. *This paper details preliminary results of the numerical modeling of the elastic curve (Euler's elastica) and three elementary bending-active structures using the Finite Element Modeling (FEM) software Ansys®. Modeled structures include variations on a single beam, a simple gridshell, and an umbrella. Results suggest bending-active structures exhibit distinct structural properties when compared to similar curves, and the choice of element type substantially affects the results of the model. Ongoing research will explore further numerical and physical modeling of more complex bending-active structures and is part of an ongoing study to further the understanding of numerical modeling in the structural design of bending-active structures.*

Keywords: *Bending-active, finite element analysis, elastic curve, gridshell, umbrella*

INTRODUCTION

Bending-active structures employ systemized large elastic deformations to create curves from initially linear or flat members. The technique of active bending has been employed throughout history as the simplest method of producing curved elements, ranging from small wicker baskets to large structures, such as gridshells and tensile membranes, with some notable advantages in fabrication and construction. However, previous form-finding techniques rely on either empirical studies of material performance or approximations of final forms through experimental form-finding methods such as hanging models. Only through contemporary advances in nonlinear FEM can bending-active structures be modeled as they are erected, including accurate large deformations due to geometric nonlinearity, material characteristics and limitations, and cumulative bending stresses (Lienhard et al. 2013). Advances in nonlinear FEM analysis of bending-active structures will allow these unique structures to reach their full structural potential through calculated load-based design.

The Mannheim Multihalle, erected in 1974, is widely regarded as the starting point of "elastic gridshells," structures formed by lifting a flat planar grid into a shell, and then fixing the shell in place. The final shape of structures such as the Mannheim are defined by "hanging models", the standard method of determining curved forms from flat forms. Recent advances in numerical modeling have made possible the inverse - flat geometry can now be derived from the desired final shape (Du Peloux et al. 2015). Aided by these advances, recent projects explore more complex bending-actives forms, such as the interaction between bending-active components and tensile membranes and bending-active structures made of composite material.

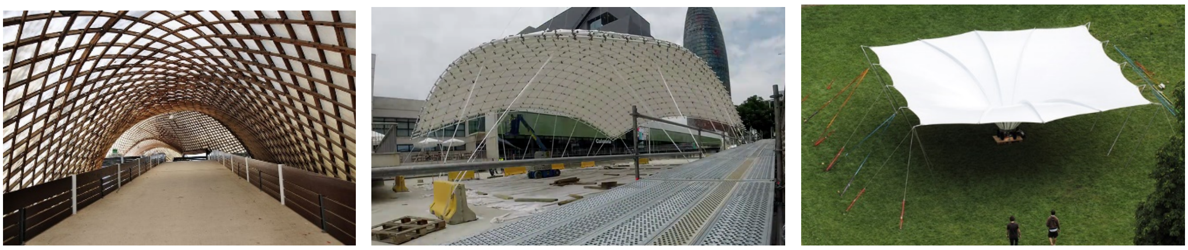

Figure 1. (a) The Mannheim Multihalle timber elastic gridshell (Berberich, 2012); (b) Elastic gridshell made of glass fiber reinforced polymer (GFRP) tubes (CODA 2017); (c) Marrakech membrane roofing made of elastically-bent fiberglass rods (Str.ucture 2011).

In this study, FEM analysis using ANSYS® Mechanical™ is conducted for the elastic curve (Euler's elastica) and three elementary structures: a single beam, a simple gridshell, and an umbrella. ANSYS® Mechanical™ is a finite element analysis (FEA) software for structural analysis developed by ANSYS, Inc. (ANSYS, Inc. 2015). The Mechanical APDL command-based user interface was selected in order to gain precise control over model parameters and increase the speed of solutions, though similar results should be achieved in the newer interfaces of ANSYS® Workbench™ and ANSYS® Aim™. All models in this paper were created with ANSYS Student, which provides a free license of ANSYS software for educational purposes.

In FEM analysis, different element types may lead to variations in results as they behave differently based on their properties. We explore the performance of models using two different element types in ANSYS, BEAM188 and SHELL181. The BEAM188 3-D Linear Finite Strain Beam is based on Timoshenko beam theory, and is a linear (2-node) beam element in 3-D with six degrees of freedom at each node. BEAM188 was chosen for modelling bending-active structures due to its effectiveness in large strain nonlinear applications. SHELL181 is a four-node, finite strain shell element, with six degrees of freedom at each node, and is also suitable for large strain nonlinear applications. The elastic curve and single beam, essentially modeled in two dimensions, are modeled only with beam elements. The gridshell, in three dimensions, is modeled with both beam and shell elements.

1 ELASTIC CURVE

A Euler elastica or elastic curve is a mathematical model for the shape assumed by a thin inextensible rod when constraints are placed at the endpoints (Brander et al. 2017). We model an elastic curve in order to gauge accuracy of ANSYS solutions by comparing them to exact elastic solutions. Campanelli et al. (2000) showed that for a cantilever beam subject to a compressive load at the free end, ANSYS can achieve 99% accuracy when the applied load corresponds to 40° to 120° of rotation of the free end.

We conduct a similar test using the most current version of ANSYS (ANSYS 18.1) by applying loads that correspond to 20° to 120° degrees of rotation in increments of 20°. Consistent with every model in this paper, we use material properties of softwood: a modulus of elasticity of $1x10^{10}$ Pa, Poisson's Ratio of 0.4, and density of 500 kg/m^3. All models are of a 10m beam with a square cross section of 0.1 m per side and meshed with an element size of 0.1 m.

1.1 Modeling Procedure

In order to control the direction of deformation, a small load must first be applied at the free end in the direction of bending. A larger load is required for larger deformations. For these deformations, a 10N load is sufficient. This load is marked "1" in Fig. 2.

The normal applied load (P) is calculated using the ratio of the critical load (P_{cr}) (Eq. 1) to the load required for the degree of deformation. Ratios, corresponding angles, and solutions can be found in Table 1. The applied load is marked "2 (P)" in Fig. 2.

$$P_{cr} = \frac{\pi^2 EI}{4l^2}. \tag{1}$$

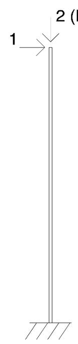

Figure 2. Elastica problem set up for a cantilever beam. 1 is a small force of 10N to direct the path of deformation. 2 is the applied load (P).

Proceedings of the XXXVIII Iberian Latin-American Congress on Computational Methods in Engineering
P.O. Faria, R.H. Lopez, L.F.F. Miguel, W.J.S. Gomes, M. Noronha (Editores), ABMEC, Florianópolis, SC, Brazil, November 5-8, 2017.

1.2 Results

Results show ANSYS 18.1 solutions are much closer to exact solutions than in the previous version of ANSYS used in Campanelli et al. (2000). ANSYS 18.1 solutions have a margin of error of approximately 0.5° or less across all loads tested. Campanelli et al. (2000) solutions have a margin of error of under 1.0° for only four values: 60°, 80°, 100°, and 120°. Both ANSYS solutions show a trend of decreasing margins of error (positive values to negative values) as the deformation increases.

Table 1. Ratios used to calculate applied load, exact solutions, ANSYS 18.1 solutions, and ANSYS solutions from Campanelli et al. (2000)

P/P_{cr}*	**1.015**	**1.063**	**1.152**	**1.293**	**1.518**	**1.884**	**2.541**
θ_{exact}	20°	40°	60°	80°	100°	120°	140°
$\theta_{ANSYS18.1}$	20.51°	40.34°	60.21°	80.16°	100.14°	120.09°	139.92°
$\theta_{Campanelli}$	33.85°	41.15°	59.80°	79.79°	99.93°	119.98°	131.84°

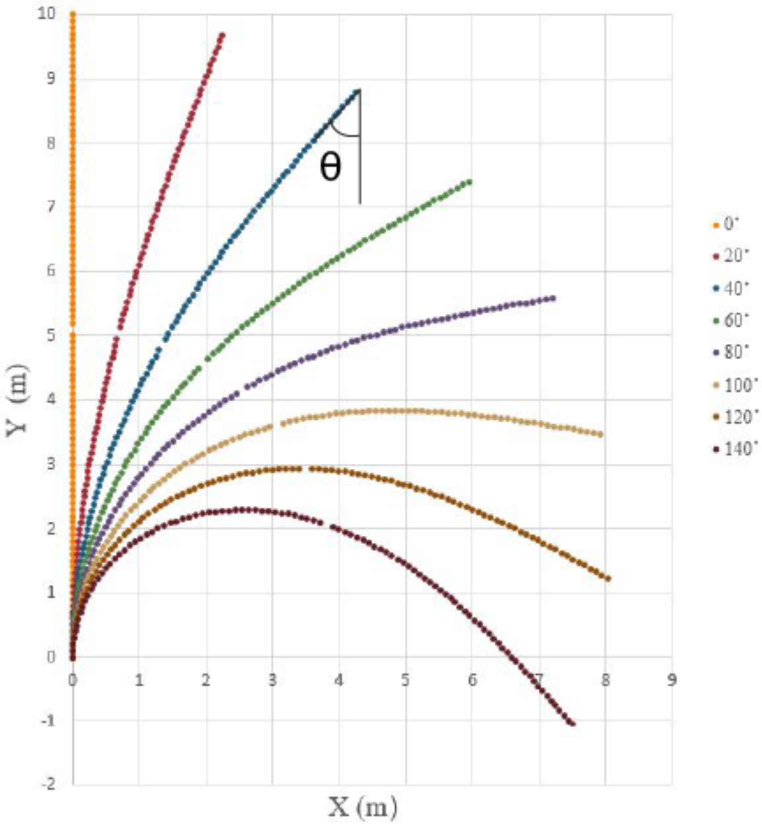

Figure 3. Elastica problem solutions in ANSYS 18.1.

2 SINGLE BEAM

An elastically deformed single beam is the basic building block of all bending-active structures. As for the elastic curve, we model the single beam using material properties of softwood (modulus of elasticity of $1x10^{10}$ Pa, Poisson's Ratio of 0.4, and density of 500 kg/m^3) and all models are of a 10m beam with a square cross section of 0.1 m per side and meshed with an element size of 0.1 m.

2.1 Modeling Procedure

The beam is first deformed to a curve by applying an upwards force of 10,000N, labeled "1" in Fig. 4, and then a normal inwards force of 10,000N, labeled "2" in Fig. 4. The upwards force is then removed. The deformed shape is then clamped in place. Transversal displacements are restrained along the beam, and the rotation along its axis is restrained at the left end, at the initial straight configuration, then released at subsequent steps, when the curvature of the beam, combined with the transversal restraints, suffice for avoiding any rigid body movement.

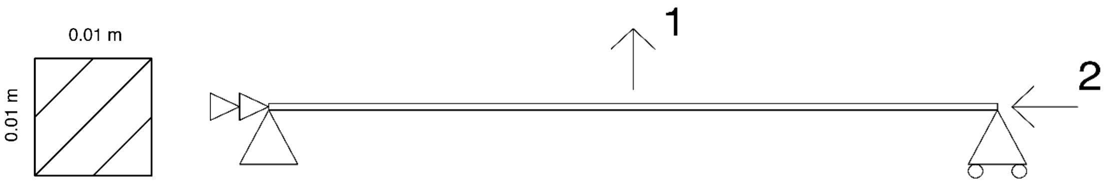

Figure 4. (a) Cross section of single beam; (b) Diagram of straight simply supported beam. Because the models are in 3D, the rotational displacement about the x-axis is fixed at the pin support. 1 is a force of 10,000N and 2 is a force of 10,000N applied to elastically deform the beam.

The resulting elastic curve represents a pre-stressed "bending-active" beam. Its performance is then compared to the performance of a "pre-cast" curved beam under three loading conditions: a concentrated force, a distributed force, and a gravity load (Fig. 5). The presence of initial stress from bending is what differentiates a bending-active structure and a "pre-cast" structure of the same shape, which was directly formed with the curved geometry.

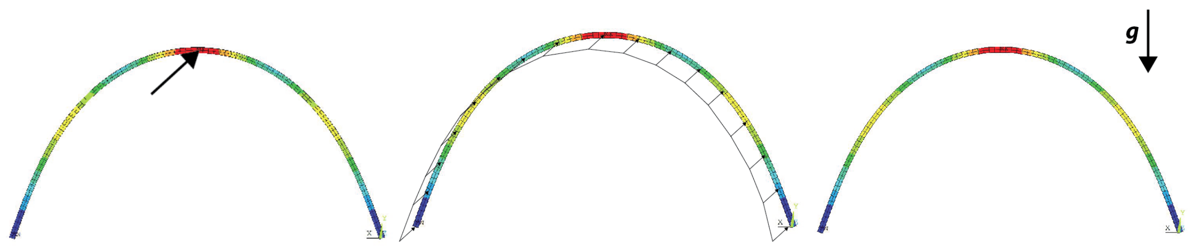

Figure 5. (a) Lateral concentrated load of 10,000N applied on curved beam; (b) Lateral "wind" load of 10,000N distributed over the length of the beam; (c) Gravity "self-weight" load over the entire beam.

In Ansys, these two structures are simulated by first extracting the deformed geometry separate from its initial stresses. A new analysis of the "bending-active" model is performed by importing both deformed geometry and initial stresses, and a new analysis of the "pre-cast" model is performed by importing only the geometry. Resulting stresses on the pre-stressed beam are then compared to resulting stresses on a beam of the same shape, with the same loading, but with no initial stresses – similar to a curve made of precast concrete or a calendered tube.

2.2 Results

The “pre-cast” models and “bending-active” show similar deformation across all three loading conditions, though “pre-cast” models showed slightly greater deformation than “bending-active” models. Figure 6 shows actual and relative deformation values for each loading. Relative deformation values are approximately 52% for “pre-cast” models and 48% for “bending-active” models; “pre-cast” models deform approximately 4% more than their corresponding “bending-active” model deforms for the same loading conditions.

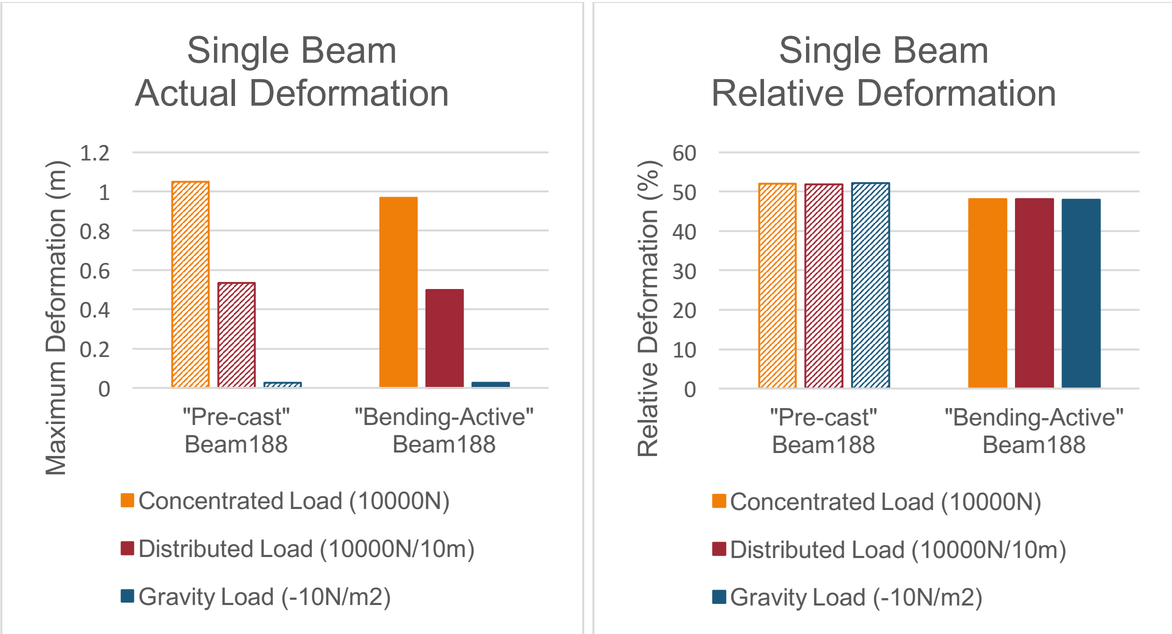

Figure 6. (a) Actual deformation of a single beam for “pre-cast” and “bending-active” models under three loading conditions; (b) Relative deformation of a single beam for “pre-cast” and “bending-active” models under three loading conditions. Relative deformation is calculated by dividing the actual deformation of a given model over the sum of the deformations of models with the same loading.

3 SIMPLE GRIDSHELL

The natural expansion of the bending-active single beam is a simple elastic gridshell composed of several interlocking beams. As with the single beam, the performance of a “bending-active” gridshell is compared to a “pre-cast” gridshell of the same shape, with an added point of comparison of the same gridshells modeled using beam elements versus shell elements. As with the elastic curve and single beam, the gridshell’s component beams have a square cross section of 0.1 m per side and material properties based on a soft wood, with a modulus of elasticity of 1x1010 Pa, Poisson’s Ratio of 0.4, and density of 500 kg/m3.

3.1 Modeling Procedure

For each model, a planar 10 m by 15 m gridshell with connections every 5 m. is deformed into a curved shell by enacting a gravity load of 50 N/m^2, resulting in the standard “hanging model” shape (Fig. 7). The curved gridshell is then fixed into place.

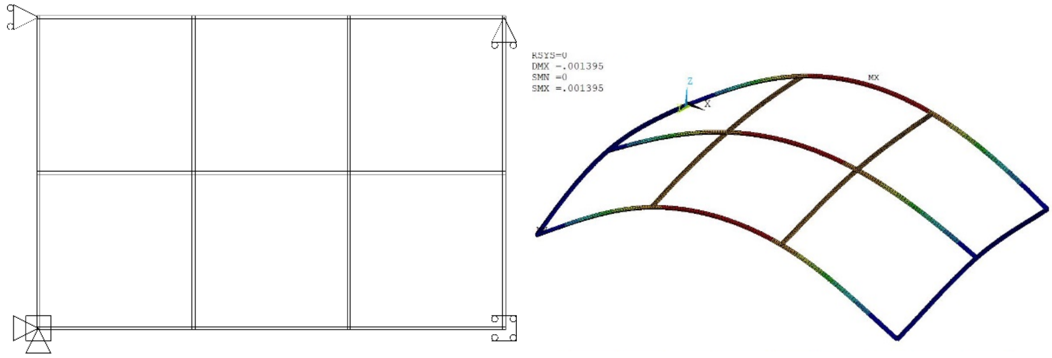

Figure 7. (a) Scale diagram of starting gridshell configuration. Bottom left corner is pinned. Top left corner is a free to move in the y-direction. Top right corner is free to move in the x-direction. Bottom right corner is free to move in the x and y-directions; (b) Deformed gridshell in “hanging model” shape. Formed by applying an upwards acceleration of 50 N/m^2.

Again, three loading conditions are used to compare the performance of a pre-stressed “bending-active” gridshell to a “pre-cast” gridshell with no initial stresses. The concentrated lateral load consists of two 20N loads applied at the center joints of the gridshell (Fig. 8a). The distributed lateral “wind” load consists of 250N even applied across one side of the grid shell (Fig. 8b). The gravity “self-weight” load is applied to represent each structure’s performance in standard conditions with no external loading.

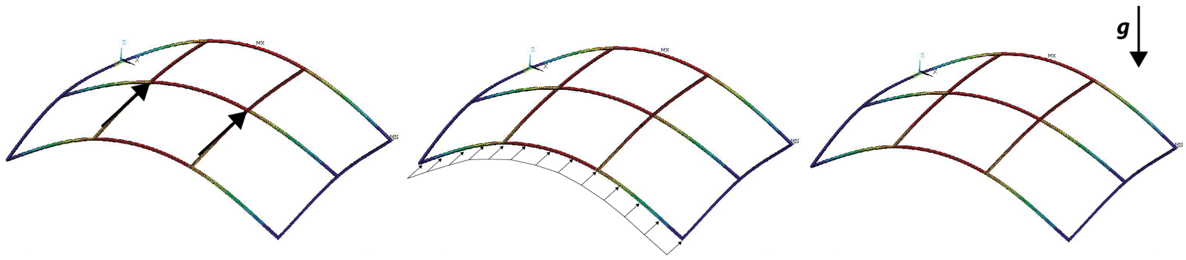

Figure 8. (a) Two lateral concentrated loads of 20N each applied on the gridshell; (b) Lateral “wind” load of 250N distributed over the length of one side of the gridshell; (c) Gravity “self-weight” load over the entire gridshell.

3.2 Results

“Pre-cast” versus “Bending-active.” All comparisons between “pre-cast” and “bending-active” gridshells showed similar trends. The “pre-cast” models showed expected deformation proportional to the load applied. The “bending-active” models, however, showed very little deformation compared to the “pre-cast” for concentrated and distributed loads, but greater deformation for the gravity load (Fig. 9a). Thus results for concentrated and distributed loads applied to the gridshell are consistent with results for the single beam but results for gravity load applied to the gridshell and single beam are inconsistent.

Beam elements versus shell elements. Results are overall similar between beam element and shell element models, with somewhat larger displacements obtained with shell element models. While the degree of magnification differed between model types and loading conditions, all comparisons consistently showed greater deformation for shell elements than for beam elements

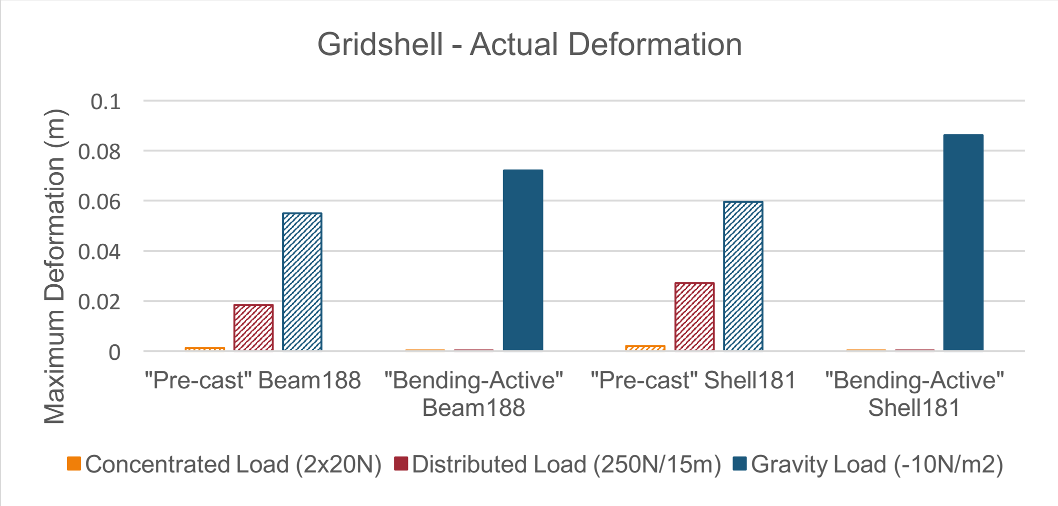

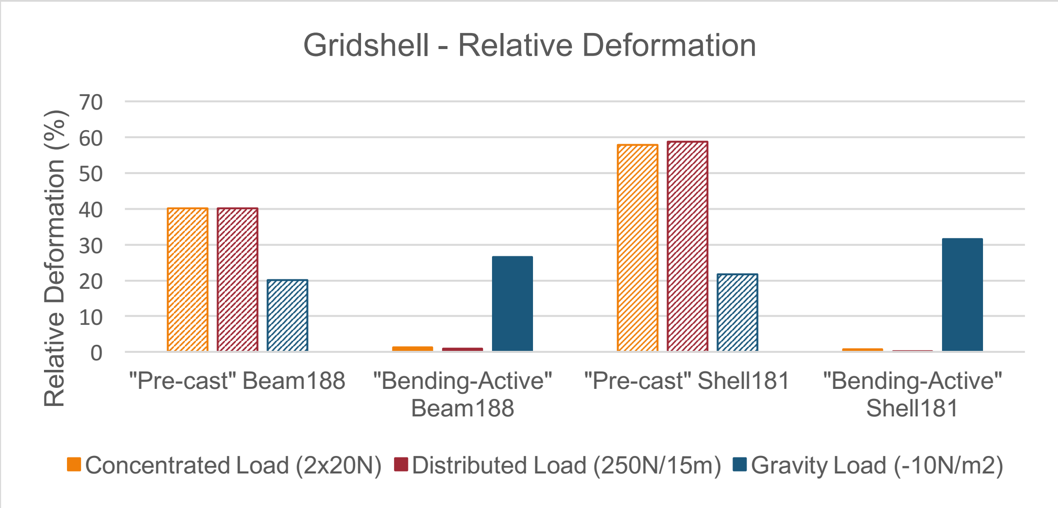

Figure 9. (a) Actual deformations of "pre-cast" and "bending-active" beam-element and shell-element gridshell models under three loading conditions; (b) Relative deformations of "pre-cast" and "bending-active" beam-element and shell-element gridshell models under three loading conditions. Relative deformation is calculated by dividing the actual deformation of a given model over the sum of the deformations of models with the same loading.

4 UMBRELLA

4.1 Modeling Procedure

Umbrellas are paradigmatic cases of bending-active structures, where the initially straight ribs are bent by the action of the membrane canopy but, reciprocally, the canopy is prestressed by the bending of the ribs. While the canopy bends the ribs, it also stabilizes them against lateral buckling, so the ribs can be remarkably slender. On the other hand, since the geometry of the ribs and the canopy depends on their mutual interaction, a viable configuration of an umbrella, comprising its geometry and its stress state cannot be arbitrarily prescribed, but must be found by some suitable procedure. Consider the umbrella shown in Fig. 10 in three different stages. In Fig. 10a the umbrella is closed, its ribs are straight, and the canopy fabric is slack. The system is a continuous mechanism, rather than a structure, and is rather difficult to model. The fabric bending stiffness must be considered, and special procedures are required to ensure convergence of a numerical model. In Fig. 10c the umbrella is fully opened, the ribs are fully bent, and the fabric canopy is fully prestressed, in a suitable membrane state. Once at the fully open stage, the umbrella behaves as a standard membrane structure, though a rather flexible one. Figure 10b shows the umbrella at an intermediate stage, when the ribs are just about to start bending, and the canopy segments are just about to start being stressed. Numerical modelling of the transition stages, from the intermediate to the fully open ones, can be treated as a nonlinear equilibrium problem, solved by the standard Newton's method, perhaps with some extra ingenuity from the analyst, to avoid numerical divergence of the model.

Figure 10. An umbrella in (a) a closed configuration; (b) an intermediate configuration; (c) a fully opened configuration.

In Fig. 11a we show the geometric parameters of an umbrella of rather arbitrary size, where geometry is adapted to the umbrella's intermediate stage. We assume that the fabric segments are perfectly flat at this configuration. We also assume that the stretchers are connected to the ribs and to the runner by revolute joints, and the runner slides along the shaft axis. Figure 11b displays the initial configuration of finite element model, which represents the umbrella at the intermediate stage. The ribs are modelled by BEAM188 elements, the canopy segments are modelled by SHELL41 membrane elements, with 'tension only' option, and each stretcher is represented by a single truss element (LINK180).

At the initial configuration, we impose a small isotropic prestress to the membrane, to achieve some geometrical stiffness and properly initialize iterations by Newton´s method, otherwise the initial tangent stiffness matrix is non-positive-defined at this configuration. Besides, if the rotation between the ribs is released, at the top notch of the model, the model also would be hypostatic. To circumvent that, we assumed that the ribs were connected at the notch end by means of flexible spring elements, yet capable of transmitting some bending and torsion moments.

The umbrella is then activated by displacing the runner vertically. In the present example, we impose a 20cm displacement, as sketched in Fig. 11c, which displays both the initial and final geometries of ribs and stretchers.

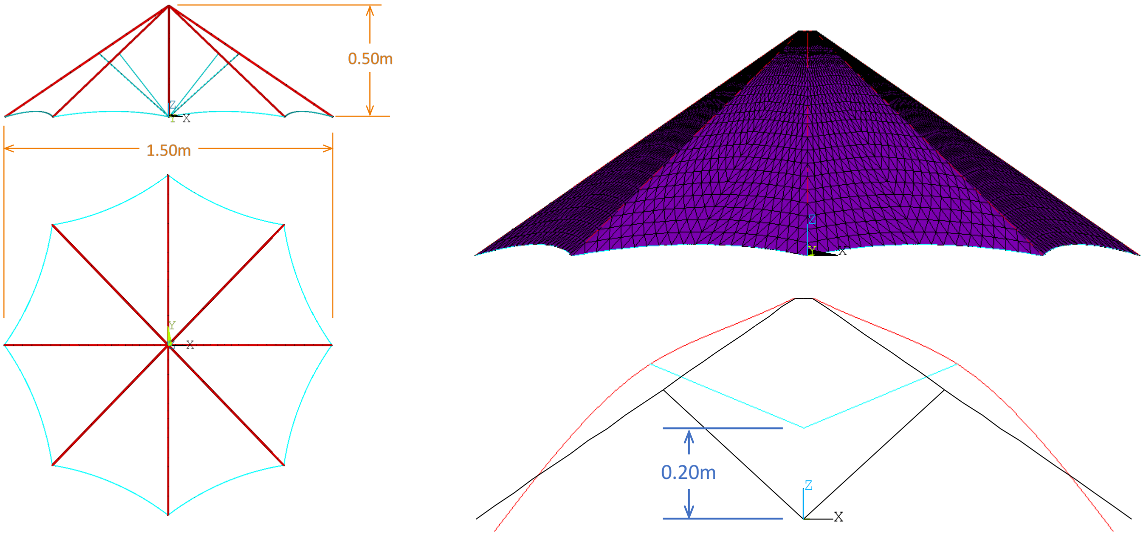

Figure 11. (a) Basic geometric parameters of an umbrella model; (b) Initial state of finite-element umbrella; (c) Displacement imposed to the runner, and resulting deformed shape of the ribs.

4.2 Results

For this preliminary example, we have loosely defined the umbrella's dimensions, materials and cross-sections of the members, so we focus on the qualitative behavior of the results, rather than on numerical values. Figure 12 shows the field of the displacement norms from the intermediate to the fully open stage, defined by a 0.2m vertical displacement of the runner. The overall deformations are qualitatively coherent, with larger curvatures observed at the juntion of the stretchers and ribs.

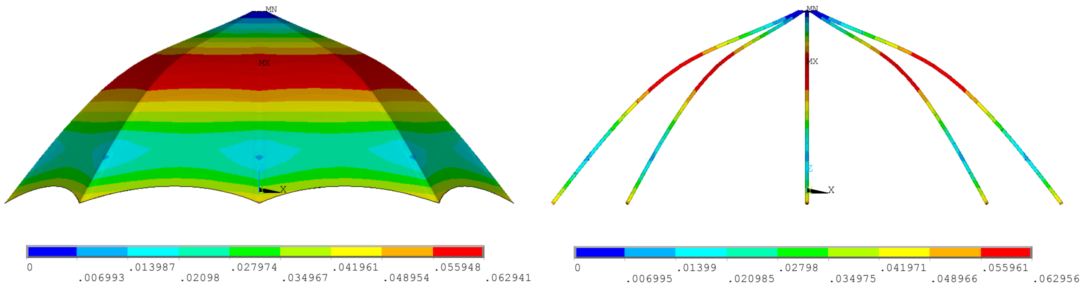

Figure 12. Field of the displacement norms (a) on the canopy membrane; (b) on the rib beams (in meters).

Some small parasitic curvature is also observed at the ribs, close to the top notch ends, indicating that the stiffness of the spring elements shuld be further reduced, if precision is at stake. Figure 13a shows the bending moments acting on the ribs, at the fully open stage. Again, it is fully coherent with the mechanical constraints, with some parasitic bending moments at the top notch ends.

Proceedings of the XXXVIII Iberian Latin-American Congress on Computational Methods in Engineering
P.O. Faria, R.H. Lopez, L.F.F. Miguel, W.J.S. Gomes, M. Noronha (Editores), ABMEC, Florianópolis, SC, Brazil, November 5-8, 2017.

Figure 13b shows the activation force at the runner (a reaction force in our numerical model). Due to the initial prestress field prescribed do the membrane, the activation force starts from a non-zero value. Some fluctuation of the activation force is observed during the first two load increments, but the curve is monotonous afterward. Due to the horizontal tangent of the activation force curve, close to the final configuration, it can be inferred that the runner is about to snap through the shaft axis – a phenomenon that sometimes annoys users of common umbrellas. In our model, however, the snap-through is constrained, because we have controlled the runner displacement, rather than imposing forces.

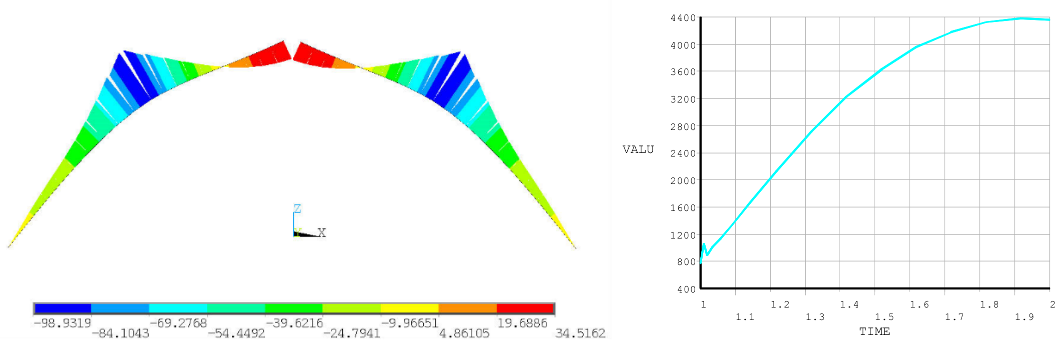

Figure 13. (a) Bending moment on the ribs, at the fully open stage (in Nm); (b) Activation force on the umbrella's runner (in Newtons).

Finally, Fig. 14 shows the fields of 1st and 2nd principal stresses at the canopy membrane at the final configuration. It is seen that the membrane tautness is uneven, with some regions presenting very low 2nd principal stress, *i.e.*, regions where the membrane is about to start to wrinkle. The membrane could be rendered tauter, with an additional patterning process – a provision seldom observed in the production of common umbrellas, but possible, if required by more exacting applications.

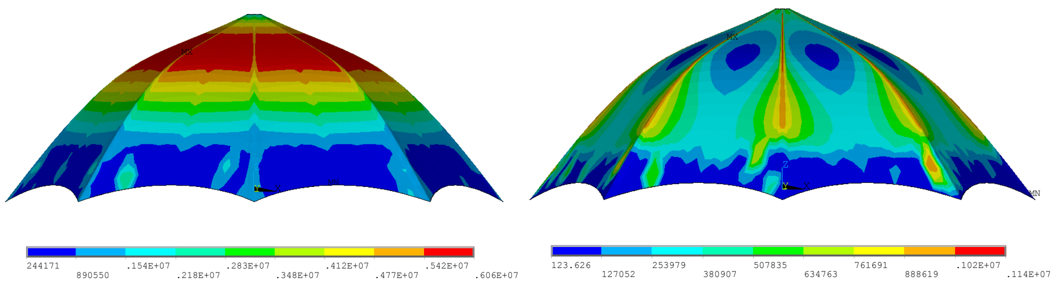

Figure 14. Fields 1st and 2nd principal stresses on the canopy membrane at the fully open stage (in N/m^2).

5 CONCLUSION

All findings in this paper are preliminary results of an ongoing study in the numerical modeling of bending-active structures.

Elastic curve. In modeling the elastic curve, our findings show that FEM software ANSYS 18.1 can calculate near exact solutions for a wide range of nonlinear, large deformation. Not only is there a minimal margin of error in our example, but our study shows significant improvements in accuracy over the past 17 years when compared to the findings of Campanelli et al. (2000), in which the authors conducted a similar study using an older version of Ansys. Further studies will conduct similar tests using ANSYS 18.1 and other FEM software on a wider range of models that require larger and more complex deformations.

Beam versus Shell Elements. The minimal difference found when modeling the gridshell in shell and beam elements is consistent with the findings of Lienhard (2014). However, a model of a twisted elastica arc in Lienhard (2014) comparing beam elements and shell elements tended to show greater deformation for the beam elements than the shell elements. Further studies will serve to pinpoint the reason for the discrepancy.

Bending-active structural stability. In modeling the beam and the gridshell, preliminary findings show a measurable difference in modeling bending-active structures and modeling their "pre-cast" forms. Specifically, for the gridshell loadings, the bending-active models exhibited less deformation for lateral loading than for gravity loading when compared to their "pre-cast" forms. This will be further tested in ongoing studies to better understand the effect of loading on bending-active structural stability. While bending-active structures today are popular for their easy of construction and economic advantages, a more detailed understanding of how bending stresses affect a structure's ability to withstand different loading conditions can lead to more efficient and effective designs. Lienhard (2014) finds that the stability of bending-active structures is dependent on stress-stiffening effects and their scaling is dependent on material elasticity and element size. Further studies will explore the effects of initial stresses in bending-active structures on more complex structures of different scales and varying material properties.

Umbrella. The modeling of the umbrella reveals complexities that arise when combining bending-active members with flexible membranes in determining appropriate material types and connections. The qualitative results of our presented model closely resemble expected behavior in common umbrellas in the displacement of the membrane and bending-active members, the activation force at the runner, and membrane tautness. Further studies will test the accuracy of quantitative results and use similar techniques to model structural scale umbrellas.

ACKNOWLEDGEMENTS

Acknowledgements

The authors would like to acknowledge the University of São Paulo – Princeton Strategic Partnership for sponsoring this collaborate transnational research endeavor.

REFERENCES

ANSYS, Inc., 2015. Ansys Student Data Sheet. Web. <http://www.ansys.com/products/academic/ansys-student>

ANSYS, Inc., 2017. Ansys 18.1 User Manual.

Berberich, H., 2012. Multihalle, Herzogenried Park, Mannheim, eastern entrance. Photograph. <https://commons.wikimedia.org/wiki/File:Multihalle10.jpg>

Brander, D., Gravesen, J. & Nørbjerg, T.B, 2017. Approximation by planar elastic curves. *Advances in Computational Mathematics*, vol. 43, n. 1, pp. 25-43.

Campanelli, M., Berzeri, M., & Shabana, A., 2000. Performance of the incremental and non-incremental finite element formulations in flexible multibody problems. *Transactions-American Society of Mechanical Engineers Journal of Mechanical Design*, vol. 122, n. 4, pp. 498-507.

CODA (Computational Design Affairs), 2017. Closca FADFest 2017. Video. <https://vimeo.com/224677582>

Du Peloux, L., Tayeb, F., Caron, J. & Baverel, O., 2015. The Ephemeral Cathedral of Créteil: a 350m2 lightweight gridshell structure made of 2 kilometers of GFRP tubes. *CIGOS 2015: "Innovations in Construction", May 2015, Cachan, France. Proceedings of CIGOS 2015.*

Lienhard, J., 2014 *Bending-Active Structures: Form-Finding Strategies Using Elastic Deformation in Static and Kinetic Systems and the Structural Potentials Therein*. PhD thesis, University of Stuttgart.

Lienhard, J., Alpermann, H., Gengnagel, C., & Jan Knippers, 2013. Active Bending, a Review on Structures Where Bending Is Used as a Self-Formation Process. *International Journal of Space*, vol. 28, no. 3–4, pp. 187–96.

Str.ucture, 2011. Bending active membrane roofing Marrakech Itke University of Stuttgart. Photograph. < http://www.str-ucture.com/en/what/research-and-development/reference/bending-active-membrane-roofing-marrakech-itke-university-of-stuttgart-2011/ >